NASA TECHNICAL NOTE

NASA TN D-3335

NASA TN D-3335

FLIGHT DEMONSTRATION OF A NOSE-MOUNTED ROTATING-SOLID-PROPELLANT ROCKET CONTROL SYSTEM AND A COMPARISON WITH ANALOG STUDIES

by Kirby H. Williams and Robert L. James, Jr.

Langley Research Center
Langley Station, Hampton, Va.

NATIONAL AERONAUTICS AND SPACE ADMINISTRATION • WASHINGTON, D. C. • MARCH 1966

FLIGHT DEMONSTRATION OF A NOSE-MOUNTED ROTATING-SOLID-PROPELLANT ROCKET CONTROL SYSTEM AND A COMPARISON WITH ANALOG STUDIES

By Kirby H. Williams and Robert L. James, Jr.

Langley Research Center
Langley Station, Hampton, Va.

NATIONAL AERONAUTICS AND SPACE ADMINISTRATION

For sale by the Clearinghouse for Federal Scientific and Technical Information
Springfield, Virginia 22151 – Price $0.55

FLIGHT DEMONSTRATION OF A NOSE-MOUNTED ROTATING-SOLID-PROPELLANT ROCKET CONTROL SYSTEM AND A COMPARISON WITH ANALOG STUDIES

By Kirby H. Williams and Robert L. James, Jr.
Langley Research Center

SUMMARY

A flight-test investigation of a space-vehicle upper stage employing a rotating-solid-rocket attitude control system is described. Experimental data received from an onboard telemetry system are presented and discussed. These data show that the control system is capable of providing three-axis control of the space-vehicle upper stage in the flight environment. Postflight analog computer studies are also presented and compared with the flight data. These results show good agreement, and thus validate the mathematical representation of the flight system.

INTRODUCTION

With the advances toward larger and more complex space vehicles there has grown a need for more versatile and efficient means of controlling them. In addition to accurate and reliable attitude control, it would be desirable to have a control system inherently capable of providing such auxiliary services as velocity control, retro-thrust, and spin-up. From a reliability standpoint as well as generality of application, it would be desirable to have a control system that can be developed independently of the main vehicle system. None of the methods presently in use is capable of providing all of these functions, and most of them engender significant performance degradation because of deadweight and excessive actuation power requirements. The most widely used control systems at present include jet vanes, jetavators, swivel nozzles, secondary injection, and reaction jets. Except for reaction jets, each of these systems must be integrated with the propulsion system.

As part of the continuing research in the field of aerospace controls by NASA, an investigation was conducted to study the control characteristics of a system possessing all of these attributes. The particular model under investigation was designed and developed under NASA contract (see ref. 1) for the George C. Marshall Space Flight Center and was integrated into a research vehicle and flight tested by the Langley Research Center. The control system consists of four small solid rockets arranged in a quadrate around the vehicle nose. Control moments are produced by rotation of the rockets about axes perpendicular

to the vehicle center line. The purpose of this report is to present the results of a flight demonstration of this control concept as applied to a space-vehicle upper stage and to provide a comparison with postflight analog-computer analyses to confirm the validity of machine simulation.

A previous demonstration of the control concept utilizing a dynamic test stand was conducted on the ground. Results of this demonstration may be found in reference 2. Detailed analyses of control-system nonlinear characteristics, determination of gains required for satisfactory control, events sequencing, etc., were made by using analog-computer facilities and are described in reference 3.

SYMBOLS

Measurements for this investigation were taken in the U.S. Customary system of Units. Equivalent values are indicated herein in the International System (SI) in the interest of promoting use of this system in future NASA reports.

A	area, square feet (meters^2)
a,b	direction cosine used in computing thrust component along missile Y- and Z-axis, respectively, dimensionless
c,d,e	moment arm for thrust moment about missile X-, Y-, and Z-axis, respectively, feet (meters)
$C_{X,0}$	axial-force coefficient at zero flow incidence angle, dimensionless
C_Z	normal-force coefficient, dimensionless
C_{Z_α}	rate of change of normal-force coefficient with angle of attack, $\frac{\partial C_Z}{\partial \alpha}$, 1/radian
C_Y	side-force coefficient, dimensionless
C_{Y_β}	rate of change of side-force coefficient with angle of sideslip, $\frac{\partial C_Y}{\partial \beta}$, 1/radian
F	nominal thrust of one control rocket multiplied by cos 10° (cant angle), pound (newtons)
$F_{X,c}, F_{Y,c}, F_{Z,c}$	control thrust along X-, Y-, and Z-axes for nominal control system operation, pound (newtons)

$F'_{X,c}, F'_{Y,c}, F'_{Z,c}$ control thrust along X-, Y-, and Z-axes for restrained control system operation, pound (newtons)

$F_{Z,ex}$ extraneous thrust along Z-axis, pound (newtons)

g acceleration due to force of gravity, feet/second^2 (meters/sec^2)

I_X, I_Y, I_Z mass moment of inertia about X-, Y-, and Z-axis, respectively, slug-feet^2 (kilogram-meter^2)

K_2 control-subsystem internal-velocity feedback gain, volts/radian/second

K_3 control-subsystem acceleration gain, radians/second^2/volt

K_p, K_q, K_r roll-, pitch-, and yaw-rate gain, volts/radian/second

K_δ control-rocket position feedback gain, volts/radian

K_ϕ, K_θ, K_ψ roll-, pitch-, and yaw-attitude gain, volts/radian

M Mach number, dimensionless

m_f frictional parameter, $\frac{\text{Frictional moment}}{\text{Inertia}}$, radians/second^2

$M_{X,c}, M_{Y,c}, M_{Z,c}$ control moment about X-, Y-, and Z-axes for nominal control system operation, foot-pound (newton-meter)

$M'_{X,c}, M'_{Y,c}, M'_{Z,c}$ control moment about X-, Y-, and Z-axes for restrained control system operation, foot-pound (newton-meter)

$M_{X,ex}, M_{Y,ex}$ extraneous moment about X- and Y-axes, foot-pound (newton-meter)

M_Y pitching moment, foot-pound (newton-meters)

M_{Y_q} rate of change of pitching moment with pitching velocity, $\frac{\partial M_Y}{\partial q}$, $\frac{\text{foot-pound}}{\text{radians/sec}} \left(\frac{\text{newton-meters}}{\text{radians/second}}\right)$

M_Z yawing moment, foot-pound (newton-meters)

M_{Z_r} rate of change of yawing moment with yawing velocity, $\frac{\partial M_Z}{\partial r}$, $\frac{\text{foot-pound}}{\text{radians/second}} \left(\frac{\text{newton-meters}}{\text{radians/second}}\right)$

m mass, slugs

m_f	frictional parameter, $\frac{\text{Frictional moment}}{\text{Inertia}}$, radians/second^2
p	rolling velocity, radians/second in equations, degrees/second in figures
q	pitching velocity, radians/second in equations, degrees/second in figures
$\bar{q}$	dynamic pressure, pound/square foot (newton/meters^2)
r	yawing velocity, radians/second in equations, degrees/second in figures
T	thrust of main rocket motor, pound (newtons)
t	time, seconds
u,v,w	component of missile linear velocity relative to nonrotating earth along X-, Y-, and Z-axis, respectively, feet/second (meters/second)
V	missile linear velocity relative to nonrotating earth, feet/second (meters/second)
V_s	speed of sound
V_δ	voltage input to control system, volts
X,Y,Z	body axes of missile, dimensionless
x,y,z	distance along body axes, feet (meters)
X_E,Y_E,Z_E	earth-fixed axes, dimensionless
x_E,y_E,z_E	distance along earth-fixed axes, feet (meters)
x_{cg}	center-of-gravity distance from nose, feet (meters)
x_{cp}	center-of-pressure distance from nose, feet (meters)
x_p	moment arm for control moment about X-axis, feet (meters)
x_p'	moment arm for extraneous moment about X-axis, feet (meters)
x_q	distance of pitch-roll control rockets from nose, feet (meters)
x_r	distance of yaw-roll control rockets from nose, feet (meters)
α	angle of attack, radians
β	angle of sideslip, radians

δ control-rocket rotation angle, radians

$\epsilon_\phi, \epsilon_\theta, \epsilon_\psi$ roll-, pitch-, and yaw-guidance-error signals, volts

η flow incidence angle, radians

θ pitch Euler angle of missile relative to earth-fixed axes, second in order of rotation, degrees

θ_R reference pitch angle relative to earth-fixed axes, degrees

θ_ϵ pitch-attitude-error angle of missile relative to gyro reference axis, degrees

ρ density, slugs/ft^3 (kilograms/meter^3)

ϕ roll Euler angle of missile relative to earth-fixed axes, third in order of rotation, degrees

ϕ_ϵ roll-attitude-error angle of missile relative to gyro reference axes, degrees

ψ yaw Euler angle of missile relative to earth-fixed axes, first in order of rotation, degrees

ψ_ϵ yaw-attitude-error angle of missile relative to gyro reference axes, degrees

Subscript:

0 initial value

Dots over symbols denote differentiation with respect to time. Primes indicate rate-gyro output. The numbers 1, 2, 3, and 4 denote control rocket number 1, 2, 3, and 4, respectively, as shown in the following sketch:

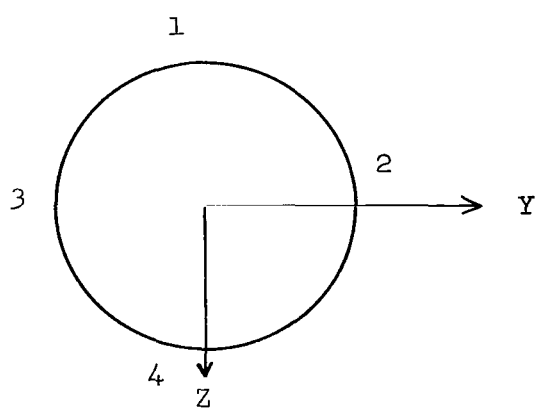

Sketch (a)-View looking forward along the X-axis.

PHYSICAL DESCRIPTION AND CHARACTERISTICS OF CONTROL SYSTEM AND RESEARCH VEHICLE

The rotating-solid-rocket control system under investigation was used to control the attitude of the upper stage of a two-stage research vehicle. In the flight application the thrust forces of the control system were used to control the stage to predetermined roll, pitch, and yaw reference attitudes by using a position- and rate-sensing guidance system to provide the necessary reference and stability functions. Each system of the vehicle is discussed subsequently in this section.

Control System

The control system under investigation is an electrical-mechanical-chemical system which utilizes the thrust of four solid-propellant rockets for control power. The control system is pictorially shown in figure 1, and schematically shown mated with the research-vehicle second stage in figure 2. The control system is compactly designed to occupy a minimum volume which necessitates the unsymmetrical location of the control rockets as seen in figure 2. The control system when fully loaded weighs 190 pounds (845 N), excluding power supplies, and consumes a maximum of 400 watts of power. The solid-propellant control rockets are bearing-mounted to allow rotation (within $\pm 60^{\circ}$ of null) about axes parallel to the Y,Z plane, and are equipped with canted nozzles that direct the thrust rearward and in planes rotated 10° from the longitudinal plane of the controlled vehicle. (See figs. 1 and 2.) The control system is geometrically arranged so that rotation of two of the control rockets produces lateral components of thrust and provides pitch controlling moments. Rotation of the remaining two control rockets produces lateral components of thrust which provide yaw controlling moments. Roll control is obtained by differential rotation of the two pitch-control rockets and by differential rotation of the two yaw-control rockets. Thus, all four control rockets are employed for roll control. With the incorporation of a predetermined program of command signals, the control system could provide vehicle spin-up; or with a $\pm 180^{\circ}$ control rocket rotational freedom could also supply vehicle retro-thrust. It must be noted, however, that the system would be capable of performing only one of the given functions (attitude control, retro-thrust, or spin-up) at any given time.

The torque necessary to rotate each control rocket is produced by an electrical drive motor and is transmitted to the control rocket through mechanical gearing. A potentiometer, which provides control-rocket position feedback, is also geared to the control rocket. The control system consists of four identical and individual loops, each composed of a control rocket, electrical drive motor, feedback potentiometer, and gearing. The nominal thrust time history for one control rocket is given in figure 3. An additional feature of the control system is that the thrust of each control rocket can be reduced at any point during its burn time. This reduction is accomplished by pyrotechnically opening a presized port directionally opposite the primary nozzle. The increased throat area results in a lower chamber pressure and thus an extension in the control-rocket burn time and a reduction in thrust. This feature could

be advantageous since it would allow a longer period of control or a vernier velocity capability. (See fig. 3.)

A more detailed discussion of the control system as a unit can be found in reference 1.

Research Vehicle

The research vehicle employed in the flight experiment is a two-stage solid-propellant rocket vehicle and is shown in figure 4. The first-stage propulsion system consists of a Castor E-8 rocket motor and two Recruit motors. The second stage consists of an Antares (X254) rocket motor (ref. 4) and a forward-mounted spacecraft. The control rockets and their vulnerable accessories are protected during the critical ascending portion of flight by four ejectable fairings. The first stage of the research vehicle is used only as a booster to place the second stage into a suitable test environment.

Second-Stage System

The second-stage system is the portion of the research vehicle which is of primary interest. As was previously indicated, only the second stage was considered to be guided by the control system. A drawing of the second stage with pertinent dimensions is given in figure 2. The second-stage nominal aerodynamic, thrust, and mass characteristics are presented in figure 5. The aerodynamic quantities are based on a reference area of 1 square foot and the Antares thrust (ref. 4) is for vacuum conditions.

The second-stage system consists of the combination of Antares and the spacecraft, and the control and guidance systems which are mounted in the spacecraft. A block diagram showing the integration of the individual systems into the complete second-stage system is presented in figure 6.

A position- and rate-monitoring proportional guidance system was employed in the research vehicle and was developed under NASA contract (ref. 5). The guidance system uses two two-degree-of-freedom gyros which provide inertial attitude information in roll, pitch, and yaw relative to a reference axis system defined by the spin vectors of the gyros. The guidance system also employs three rate gyros which are fixed in the spacecraft to measure body rates. The outputs of each gyro and the position feedback of the control rockets are weighted and appropriately summed to provide error signals to the control system (fig. 6). The numerical values and procedure for the weighting and summing are described in reference 3.

An FM/FM telemetry system located in the spacecraft was employed to monitor the desired performance parameters and to transmit these data to ground receiving stations. The system was typical of units employed in sounding-rocket flight-test research. The parameters monitored by the telemetry system are:

(1) Roll, pitch, and yaw body rates from rate gyros in the guidance system

(2) Roll-, pitch-, and yaw-attitude error angles from attitude gyros in the guidance system

(3) Rotational position of each control rocket.

RESEARCH VEHICLE TRAJECTORY AND FLIGHT EVENTS

The research-vehicle trajectory parameters as obtained from radar tracking data are presented in figure 7. Selected flight events are included in this figure for reference but a more detailed listing of the events is included in table I.

There were two malfunctions which occurred in the flight which caused deviations from the planned test sequence. The first occurred at the time of fairing separation when only three of the four fairings ejected. As a result of this malfunction, control motor number 3 was restrained from rotation during the entire test and, since the fairing was covering this motor, the thrust force imparted to the vehicle by this motor was essentially zero. A detailed treatment of the effect of this restraint on the equations of motion is included in the appendix.

Late in the burning period of the Antares motor, another vehicle malfunction which resulted in a premature burnout of this stage occurred. At this time a large disturbance of the vehicle occurred and temporarily overpowered the control system. The resulting motion of the vehicle and control system response is discussed subsequently.

RESULTS AND DISCUSSION

Flight-Test Results

Control of the research vehicle began soon after separation of the first stage. (Control rocket ignition occurred before separation but no command signals were transmitted until after separation.) This 2.3-second interval (table I) during which the control rockets were alined at the null position (fig. 8(b)) and no significant control moments were produced was programed to allow time for all four rockets to reach the same thrust level before any control maneuvers were attempted. The control period is divided into two phases. The first phase, referred to as roll control, began at a flight time of 79.9 seconds (20.1 seconds prior to second-stage ignition); the second phase, three-axis control, was initiated at 94.8 seconds and lasted the remainder of the flight. (See table I.) During roll control the vehicle is subject to roll attitude and rate control and pitch- and yaw-rate control. Later, during three-axis control, the vehicle is controlled in attitude and rate about all three axes, roll, pitch, and yaw. A detailed discussion defining the requirements for this sequencing may be found in reference 3.

Roll control.- The purpose of the roll-control phase is to reduce any existing roll rate to zero and to orient the vehicle's attitude to zero in roll. During this period, the vehicle pitch and yaw rates are controlled to zero; thus, excessive change in the pitch and yaw attitude is prevented. Figure 8 shows plots of the variation of vehicle attitudes, rates, and control-rocket rotation angles with time. It is seen from figure 8(a) that at initiation of the roll-control maneuver, the roll rate and roll attitude were both above the guidance system limit ($\pm 40^\circ$/sec for rate gyros, $\pm 30^\circ$ for attitude gyros); therefore, they had to be calculated. Roll rate was calculated from the slope of the roll-attitude curve. Roll attitude was then found by extrapolation of the attitude curve to the proper time. It should be noted (fig. 8) that insofar as the output of the roll attitude gyro is concerned, an attitude of 180° is exactly the same as 0°; 190°, as -10°; 170°, as 10°, etc.; that is, the inverse sine function is double-valued. (See eq. (A27).) At initiation of the roll-control maneuver, the vehicle had a roll velocity of 75°/sec and a roll attitude of approximately 92°. With the three control motors rotated nearly full scale, as at $t = 80.5$ seconds, a large negative moment was imparted to the vehicle, and the positive rate was reduced from 75°/sec to approximately zero in 2 seconds. The roll attitude during this time changed from 92° to 180°. At an attitude of 180°, the vehicle was unstable and the slight change in attitude brought about by the small residual roll rate resulted in the development of a positive roll moment and the subsequent orientation of the vehicle to zero attitude. At approximately 94 seconds, the roll rate and attitude were brought within 2°/sec and 2°, respectively; thus, the roll control phase was essentially completed.

Three-axis control.- At 94.8 seconds after launch, the error signals for pitch and yaw attitude were included in the control-system driving functions (eqs. (A32) to (A35)) to initiate the second phase of controlled flight, three-axis rate and attitude control. Errors of approximately 20° and -10° existed, respectively, in pitch and yaw at this time. Control moments along these axes were produced immediately, and these moments brought the vehicle toward the zero attitude. From figure 8(a) it is seen that the time required for yaw control is of the same order as that for pitch even though the initial yaw error was only one-half that of pitch; this difference arose from the fact that control motor no. 3, a yaw control motor, was restrained from rotating and, consequently, from producing any yaw control moments. This lack of control power in yaw coupled with extraneous pitch moments from the yaw-motor restraint (appendix) caused the vehicle to overshoot the reference attitude several times before being stabilized near zero. Second-stage ignition, occurring at $t = 100$ seconds, presented little or no difficulty for the control system. Stabilization of the vehicle near zero attitude about all axes was accomplished in approximately 7 seconds and was maintained within $\pm 2.5^\circ$ bounds until 131.9 seconds.

At this point the second-stage propulsion unit malfunctioned and imparted to the vehicle a series of large disturbances. These disturbances overpowered the control system momentarily and caused a severe disruption of controlled flight. (See fig. 8(a).) However, the control system recovered the vehicle from the large initial disturbance and it appears that it would have damped the motions out entirely had not thrust reduction occurred as planned at 142.3 seconds. This reduction of thrust extended the control-rocket burning time to

approximately 169 seconds. However, since only three control motors were providing control moments and these motors were operating at the lower thrust level of 5 pounds (22.24 N) (fig. 3), loss of attitude control resulted.

Analog Simulation Results

After the flight of the Vector research vehicle, an analog computer study was performed for the portion of controlled flight prior to second-stage malfunction. This study consisted of (1) simulating the flight motions and attitudes that the vehicle actually experienced, that is, with the control restraints, and (2) simulating the motions and attitudes as they would have occurred had the control system not been restrained. To make these simulations, a set of equations describing vehicle motions, guidance system outputs, control system operation, trajectory parameters, etc., were programed in a closed loop on the analog computer and the various initial conditions supplied from telemetry and radar data. The equations for making the simulations noted in part (2) are the same as those given in reference 3 and are listed for convenience in the appendix. To make the simulations noted in part (1), these equations had to be modified to take into account the restraints on the control system. These modifications are derived in the appendix.

It must be pointed out that because of the impossibility of predicting or determining the exact time history of some of the parameters of the problem, and because of errors in assigning initial conditions, an exact simulation in every detail cannot be made. General trends of motion can, however, be simulated. This simulation was made after the flight, and the results are presented here as comparisons with the flight results.

Roll control.- Figure 9(a) shows the comparison of simulated roll attitude errors with the actual flight values. Good agreement was achieved, in that the simulation follows closely the general trend of the flight data. Time of transit of the vehicle from one gyro limit to the other is the same in both cases and stabilization of the vehicle at near zero attitude occurs at approximately the same time for both cases. Figure 10 shows a comparison between the flight data and the simulation of the motions and attitudes as they would have occurred had the control system not been restrained.

Three-axis control.- At a flight time of $t = 94.8$ seconds, the program was stopped and new initial conditions were supplied for the initiation of the second phase of controlled flight. (See fig. 9(a).) The frequencies and amplitudes of oscillatory motions agree very well, especially in roll and yaw, although exact coincidence of the curves does not occur. As noted previously, the overshoots in pitch and yaw arose from the lack of control power in yaw and the development of extraneous moments in pitch. (See appendix.) If all four motors had been functioning properly, as in the simulations shown in figure 10, there would have been no extraneous moments in the equations and pitch and yaw errors would have been brought to zero very smoothly with little or no overshoot and would have been held at zero for the entire test. Roll attitude would have been controlled to within 1° for the duration of the test. Total time required

for vehicle stabilization would have been about 3 seconds as compared with 7 seconds for the three-motor operative case in actual flight.

CONCLUDING REMARKS

A new concept in rocket-vehicle attitude control has been successfully demonstrated on a space-vehicle upper stage. The particular system under investigation utilizes the thrust of four auxiliary solid rocket motors for its control power; control moments about the vehicle axes may be produced by rotation of the motors from their null position. Velocity control, spin-up, and retrothrust can also be incorporated into this system.

Controlled flight of the research vehicle was initiated by capturing a moderate roll rate accumulated during first-stage thrust and coast, and by orienting the vehicle in a roll sense to its reference attitude. This maneuver was accomplished within the allotted time of 15 seconds even though only three of the four control rockets were functioning properly.

Immediately after the stabilization of the vehicle at its reference attitude in roll, the control of vehicle attitudes about the two remaining axes was initiated. Initial errors in pitch and yaw were reduced in nominal fashion but the lack of control power from rocket no. 3 allowed the vehicle to overshoot the reference attitude. Stabilization of vehicle attitudes about all three axes was maintained within $\pm 2.5^{\circ}$ of zero until a malfunction of the research-vehicle propulsion unit imparted large disturbances to the vehicle and overpowered the control system. However, these motions were being significantly damped when thrust reduction effectively removed control-system moment-producing capability. Computer simulations show that if all four motors had functioned properly, the vehicle attitude for all axes would have been held within $\pm 1^{\circ}$ of zero until second-stage malfunction.

Postflight analog-computer simulations show good agreement with data obtained from the actual flight; thereby the validity of a mathematical model of the research vehicle was confirmed, and the feasibility of reliably simulating the flight of space vehicles utilizing this type of control system was verified.

Langley Research Center,
National Aeronautics and Space Administration,
Langley Station, Hampton, Va., December 2, 1965.

APPENDIX

EQUATIONS DESCRIBING VEHICLE AND TRAJECTORY SIMULATION FOR UNRESTRAINED AND RESTRAINED CONTROL SYSTEM

Basic Equations

This appendix is concerned with defining the effects on vehicle dynamics of altering in some way the performance of one of the control rockets. In each of the vehicle equations of motion, the control-system contributions are modified to account for the restraint on the control motor. Equations from reference 3 describing the simulation for unrestrained control system operation are repeated for convenience.

$$m\dot{u} - mvr + mwq = F(\cos \delta_1 + \cos \delta_2 + \cos \delta_3 + \cos \delta_4) + T - mg \sin \theta + C_{X,0}\bar{q}A \tag{A1}$$

$$m\dot{v} - mwp + mur = -F(\sin \delta_1 + \sin \delta_3) + Ta + mg \sin \phi \cos \theta + C_{Y_\beta}\beta\bar{q}A \tag{A2}$$

$$m\dot{w} - muq + mvp = F(\sin \delta_2 + \sin \delta_4) + Tb + mg \cos \phi \cos \theta + C_{Z_\alpha}\alpha\bar{q}A \tag{A3}$$

$$\dot{p}I_X = -F(\sin \delta_1 - \sin \delta_3 - \sin \delta_2 + \sin \delta_4)x_p + Tc \tag{A4}$$

$$\dot{q}I_Y + rpI_X - rpI_Z = -F(\sin \delta_2 + \sin \delta_4)(x_{cg} - x_q) + Td + M_{Y_q}q - C_{Z_\alpha}\alpha\bar{q}A(x_{cg} - x_{cp}) \tag{A5}$$

$$\dot{r}I_Z + pqI_Y - pqI_X = -F(\sin \delta_1 + \sin \delta_3)(x_{cg} - x_r) + Te + M_{Z_r}r + C_{Y_\beta}\beta\bar{q}A(x_{cg} - x_{cp}) \tag{A6}$$

$$\alpha = \frac{w}{u} \tag{A7}$$

$$\beta = \frac{v}{u} \tag{A8}$$

$$\eta = \frac{\sqrt{v^2 + w^2}}{u} \tag{A9}$$

$$\bar{q} = \frac{1}{2}\rho V^2 \tag{A10}$$

$$V = \sqrt{u^2 + v^2 + w^2} \tag{A11}$$

$$M = \frac{V}{V_s} \tag{A12}$$

$$\dot{\psi} = \frac{q \sin \phi + r \cos \phi}{\cos \theta} \tag{A13}$$

$$\dot{\phi} = p + \dot{\psi} \sin \theta \tag{A14}$$

$$\dot{\theta} = q \cos \phi - r \sin \phi \tag{A15}$$

$$\psi = \int_t \dot{\psi}\, dt + \psi_0 \tag{A16}$$

$$\phi = \int_t \dot{\phi}\, dt + \phi_0 \tag{A17}$$

$$\theta = \int_t \dot{\theta}\, dt + \theta_0 \tag{A18}$$

$$\dot{x}_E = u(\cos \theta \cos \psi) + v(\cos \psi \sin \phi \sin \theta - \sin \psi \cos \phi) + w(\cos \psi \cos \phi \sin \theta + \sin \psi \sin \phi) \tag{A19}$$

APPENDIX

$$\dot{y}_E = u(\cos\theta \sin\psi) + v(\sin\psi \sin\phi \sin\theta + \cos\psi \cos\phi) + w(\sin\psi \cos\phi \sin\theta - \cos\psi \sin\phi) \tag{A20}$$

$$\dot{z}_E = -u(\sin\theta) + v(\sin\phi \cos\theta) + w(\cos\theta \cos\phi) \tag{A21}$$

$$x_E = \int_t \dot{x}_E \, dt + x_{E,0} \tag{A22}$$

$$y_E = \int_t \dot{y}_E \, dt + y_{E,0} \tag{A23}$$

$$z_E = \int_t \dot{z}_E \, dt + z_{E,0} \tag{A24}$$

$$\sin\theta_\epsilon = \sin\theta \cos\theta_R - \cos\theta \cos\psi \sin\theta_R \tag{A25}$$

$$\sin\psi_\epsilon = \cos\theta \sin\psi \tag{A26}$$

$$\sin\phi_\epsilon \cos\theta_\epsilon = \sin\phi \sin\theta \cos\psi \sin\theta_R - \cos\phi \sin\psi \sin\theta_R + \sin\phi \cos\theta \cos\theta_R \tag{A27}$$

$$\ddot{\delta} + K_2K_3\dot{\delta} - m_f = K_3V_\delta \tag{A28}$$

$$\epsilon_\psi = K_r r' + K_\psi \sin\psi_\epsilon \tag{A29}$$

$$\epsilon_\theta = K_q q' + K_\theta \sin\theta_\epsilon \tag{A30}$$

$$\epsilon_\phi = K_p p' + K_\phi \sin\phi_\epsilon \tag{A31}$$

$$V_{\delta_1} = \epsilon_\psi + \epsilon_\phi - K_\delta\delta_1 \tag{A32}$$

$$V_{\delta_2} = \epsilon_\theta - \epsilon_\phi - K_\delta \delta_2 \tag{A33}$$

$$V_{\delta_3} = \epsilon_\psi - \epsilon_\phi - K_\delta \delta_3 \tag{A34}$$

$$V_{\delta_4} = \epsilon_\theta + \epsilon_\phi - K_\delta \delta_4 \tag{A35}$$

The primes over the rates r, q, and p in equations (A29), (A30), and (A31), respectively, denote body rates less than or equal to saturation value. Rates greater than saturation value appear as saturation value to the guidance system. (See ref. 3, p. 15.)

Modifications

The nonejection of the no. 3 control rocket fairing resulted in two restraints being placed on that control rocket: (1) retention of the control rocket at the null position, and (2) reduction of the effective thrust to zero.

The following analysis describes the way in which the force and moment equations for nominal control-system operation must be modified to account for the restraints on control rocket no. 3. Although the analysis is applied to restraints on no. 3 rocket, it should be noted that the same general consequences would arise from a similar alteration of one of the other motors.

In the equations of motion (eqs. (A1) to (A6)) the term F denotes the component of control-rocket thrust in planes perpendicular to the Y- and Z-axes of the vehicle; that is, the product of nominal control-rocket thrust and cos 10°, where 10° is the cant angle of the rocket from the longitudinal axis of the vehicle.

Multiplication of the quantity F by the cosine of the control rocket rotation angle δ gives the thrust component of that motor in the direction of the vehicle's X-axis. For nominal operation of all control motors, the total thrust in the x-direction due to the control system is:

$$F_{X,c} = F(\cos \delta_1 + \cos \delta_2 + \cos \delta_3 + \cos \delta_4) \tag{A36}$$

With motor no. 3 restrained from any rotation and from thrusting, equation (A36) becomes

$$F'_{X,c} = F(\cos \delta_1 + \cos \delta_2 + \cos \delta_4) \tag{A37}$$

APPENDIX

Multiplication of F by the sine of the rotation angle of a control rocket gives the thrust component of that motor in the lateral direction. For nominal operation then, the total thrust along the vehicle Y-axis is:

$$F_{Y,c} = -F(\sin \delta_1 + \sin \delta_3) \tag{A38}$$

(The minus sign is inserted to insure that rotation of the control motor will give a thrust component in the desired direction.)

If motor no. 3 is restrained from rotation, equation (A38) becomes simply

$$F'_{Y,c} = -F \sin \delta_1 \tag{A39}$$

The total thrust in the z-direction is, for nominal control system operation,

$$F_{Z,c} = F(\sin \delta_2 + \sin \delta_4) \tag{A40}$$

With the restraints on motor no. 3, there is an additional force in the z-direction given by:

$$F_{Z,ex} = (F_1) \sin 10^\circ \tag{A41}$$

(See sketch (b).)

The multiplication of the lateral thrust of a control motor by the roll moment arm x_p gives the contribution of that motor to the total moment about the X-axis. For nominal operation of all four control motors, the total roll-control moment is:

$$M_{X,c} = -F(\sin \delta_1 - \sin \delta_3 - \sin \delta_2 + \sin \delta_4) x_p \tag{A42}$$

With the restraints on motor no. 3, the total roll-control moment is:

$$M'_{X,c} = -F(\sin \delta_1 - \sin \delta_2 + \sin \delta_4) x_p + F_2 x_p' \sin 10^\circ \tag{A43}$$

APPENDIX

Because of the offset geometry (sketch (b)), the thrust of each control rocket produces a moment in the roll direction; under nominal conditions, these moments add up to zero

$$M_{X,ex} = x_p'(-F_1 + F_2 - F_3 + F_4)\sin 10^\circ = 0 \qquad (A44)$$

but, for $F_3 = 0$, equation (A44) becomes

$$M_{X,ex} = F_2 x_p' \sin 10^\circ$$

as in equation (A43).

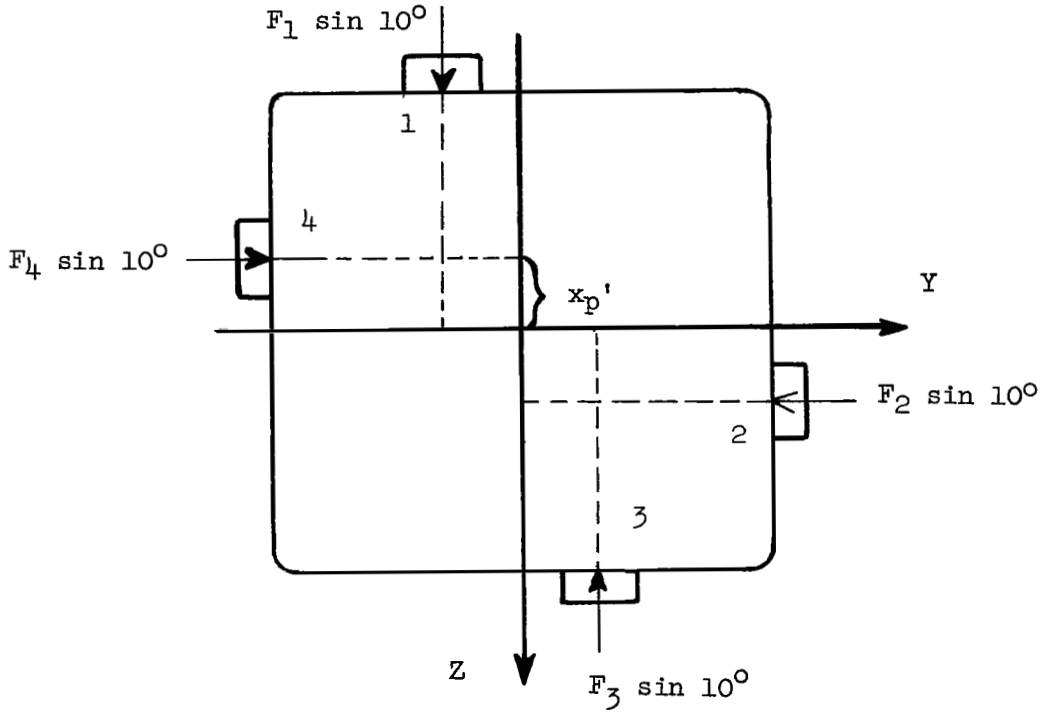

Sketch (b) - View looking forward, along positive X-axis.

The total pitch-control moment for nominal control-system operation is:

$$M_{Y,c} = -F(\sin \delta_2 + \sin \delta_4)(x_{cg} - x_q) \qquad (A45)$$

APPENDIX

The restraints on the control system result in the development of an extraneous moment in pitch which must be added to equation (A45). This additional moment arises from the imbalance between motors nos. 1 and 3 (as shown in sketch (c)) and is given by

$$M_{Y,ex} = -F_1 \sin 10^\circ (x_{cg} - x_r) - F_1 x_p \cos \delta_1 \cos 10^\circ \qquad (A46)$$

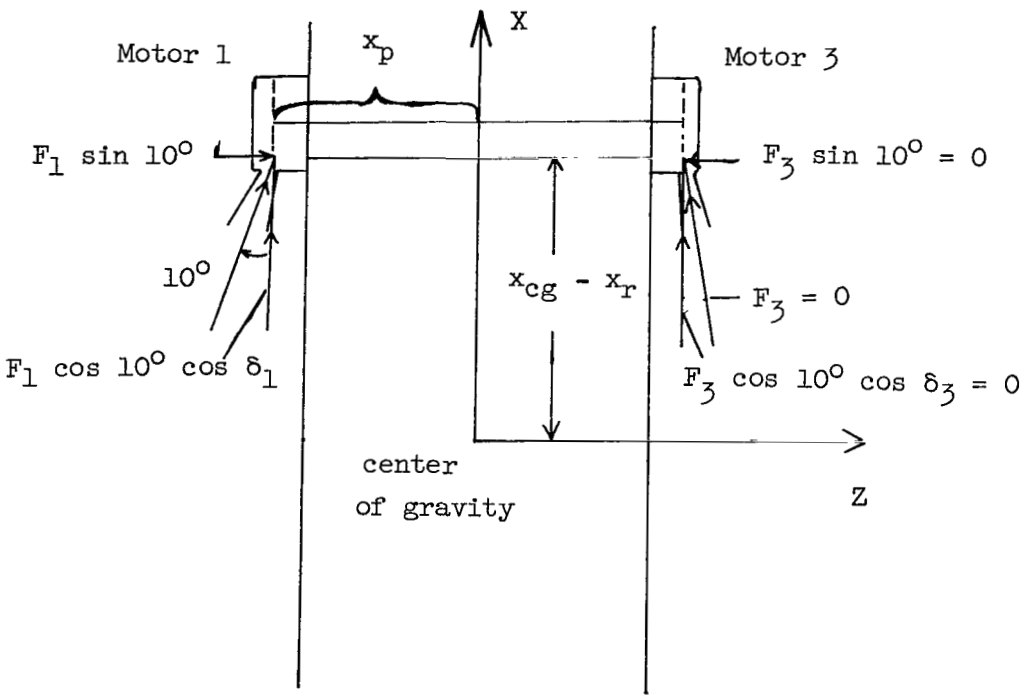

Sketch (c)

With the yaw control motors functioning properly, the yaw-control moment is given by:

$$M_{Z,c} = -F(\sin \delta_1 + \sin \delta_3)(x_{cg} - x_r) \qquad (A47)$$

When motor no. 3 is not free to rotate, this equation becomes simply

$$M'_{Z,c} = -F(\sin \delta_1)(x_{cg} - x_r) \qquad (A48)$$

APPENDIX

To make the simulations presented in this report, the thrust and rotation angle of control rocket no. 3 were considered to be zero. The complete equations describing the vehicle simulation for this modified system are

$$m\dot{u} - mvr + mwq = F(\cos \delta_1 + \cos \delta_2 + \cos \delta_4) + T - mg \sin \theta + C_{X,0}\bar{q}A \tag{A49}$$

$$m\dot{v} - mwp + mur = -F(\sin \delta_1) + Ta + mg \sin \phi \cos \theta + C_{Y_\beta}\beta\bar{q}A \tag{A50}$$

$$m\dot{w} - muq + mvp = F(\sin \delta_2 + \sin \delta_4) + F_1 \sin 10^\circ + Tb + mg \cos \phi \cos \theta + C_{Z_\alpha}\alpha\bar{q}A \tag{A51}$$

$$\dot{p}I_X = -F(\sin \delta_1 - \sin \delta_2 + \sin \delta_4)x_p + F_2 x_p' \sin 10^\circ + Tc \tag{A52}$$

$$\dot{q}I_Y + rpI_X - rpI_Z = -F(\sin \delta_2 + \sin \delta_4)(x_{cg} - x_q) - F_1 \sin 10^\circ(x_{cg} - x_r) - F_1 x_p \cos \delta_1 \cos 10^\circ + Td + M_{Y_q}q - C_{Z_\alpha}\alpha\bar{q}A(x_{cg} - x_{cp}) \tag{A53}$$

$$\dot{r}I_Z + pqI_Y - pqI_X = -F(\sin \delta_1)(x_{cg} - x_r) + Te + M_{Z_r}r + C_{Y_\beta}\beta\bar{q}A(x_{cg} - x_{cp}) \tag{A54}$$

REFERENCES

1. Wagle, J. A.: Final Report of ALL/TROL Control System for Project Vector A-1. EDR 4221 (Contract No. NAS 8-5045), Allison Div., General Motors, 1965.

2. Young, A. Thomas; and James, Robert L., Jr.: Test Stand Study of a Vehicle Upper Stage Employing a Rotating-Solid-Rocket Attitude Control System and a Comparison With Analog Studies. NASA TN D-2997, 1965.

3. Young, A. Thomas; and Harris, Jack E.: An Analog Study of a Rotating-Solid-Rocket Control System and Its Application to Attitude Control of a Space-Vehicle Upper Stage. NASA TN D-2366, 1964.

4. Baldwin, R. H.; Kuebeler, G. C.; Adams, W. J.; and Rubin, M. B.: Data Summary Report X254 Rocket Motor Performance. ABL/I-20 (Contract NOrd 16640), Allegany Ballistics Lab., Hercules Powder Co., Aug. 1963.

5. Anon.: Final Summary Report on Project Vector Guidance Subsystems. SGC 297R-15 (Contract No. NAS 1-2323), Space-General Corp., Feb. 25, 1964.

TABLE I.- SEQUENCE OF FLIGHT EVENTS

Event:	Flight time, sec
Torque gyros	-4.4
Ignition of Castor engine	0.1
Ignition of Recruit engines	0.3
Burnout of Recruit engines	2.6
Burnout of Castor engine	41.7
Ejection of fairings	72.6
Alinement of control rockets	75.8
Ignition of control rockets	77.6
First-stage separation	79.6
Roll control initiated	79.9
Three-axis control initiated	94.8
Ignition of Antares engine	100.0
Malfunction and burnout of Antares engine	131.9
Reduction of control rocket thrust	142.3
Burnout of control rockets	168.6

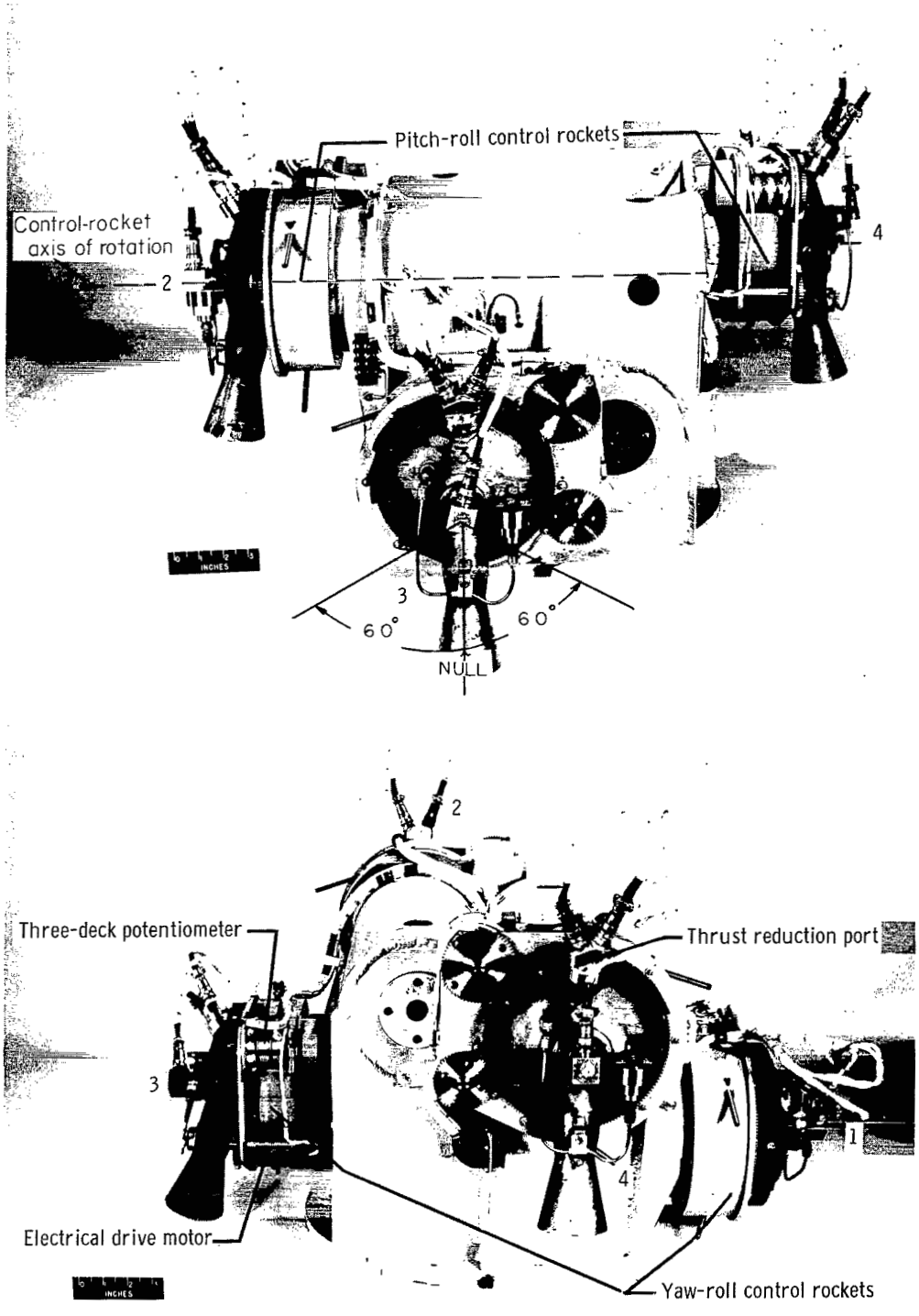

L-65-9036

Figure 1.- Photograph of control system. Numbers designate control rockets.

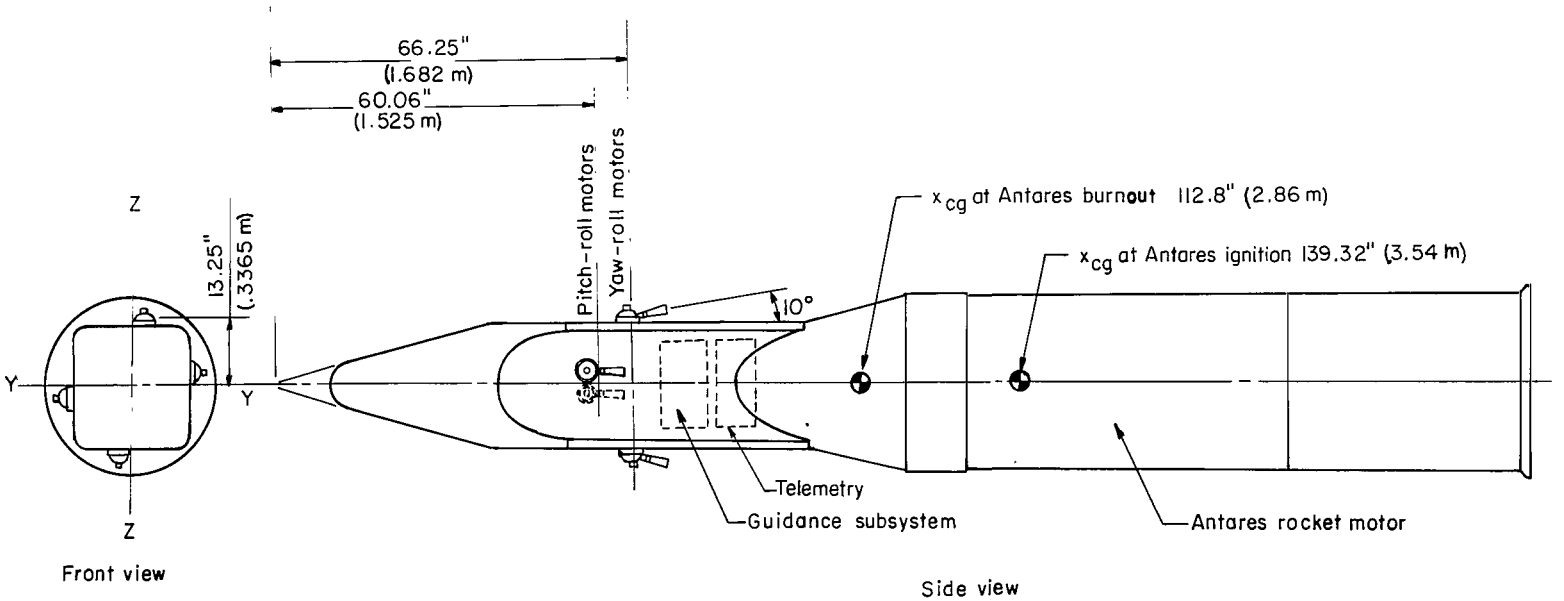

Figure 2.- Research-vehicle second stage. X_{cg} is measured relative to theoretical nose.

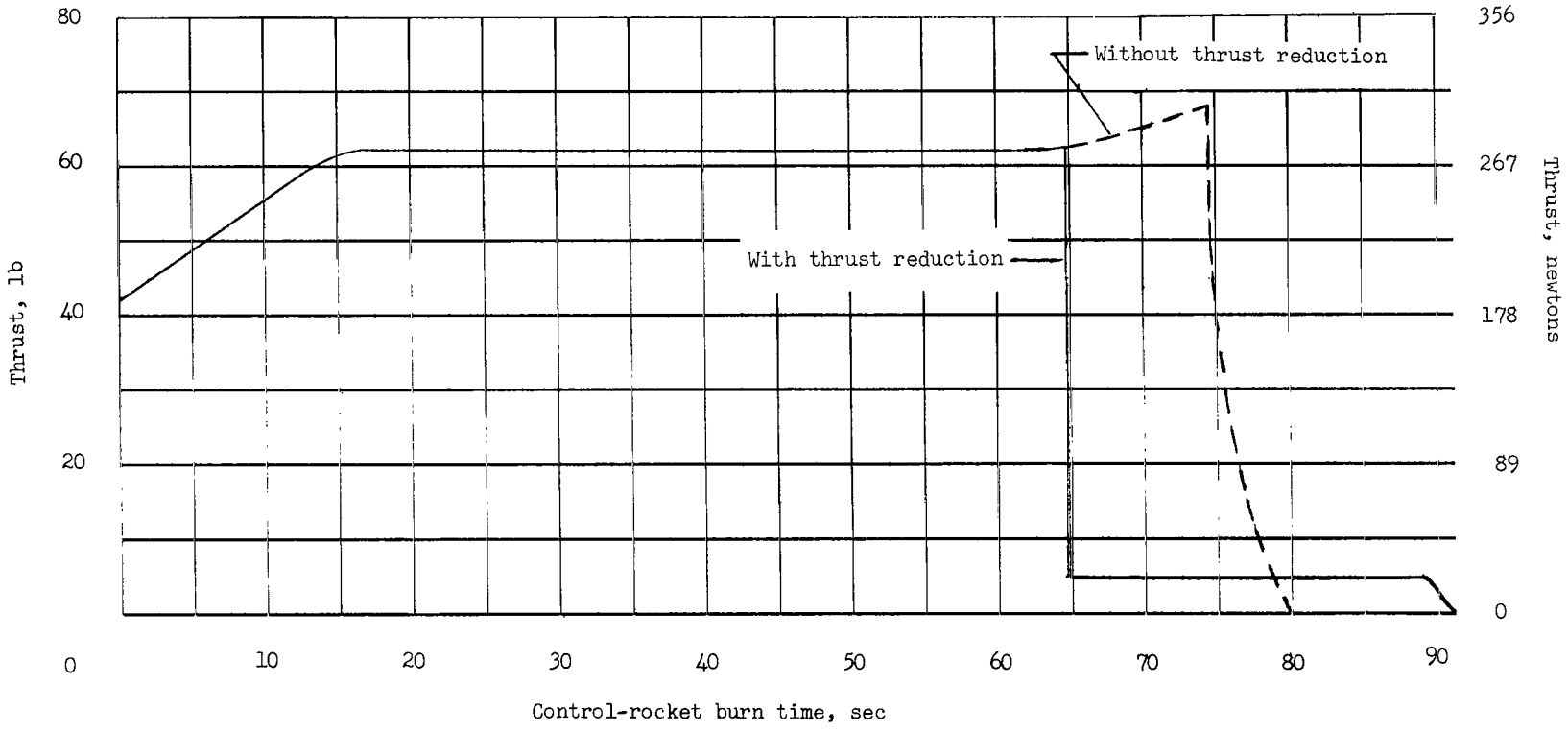

Figure 3.- Nominal thrust time history for one control rocket.

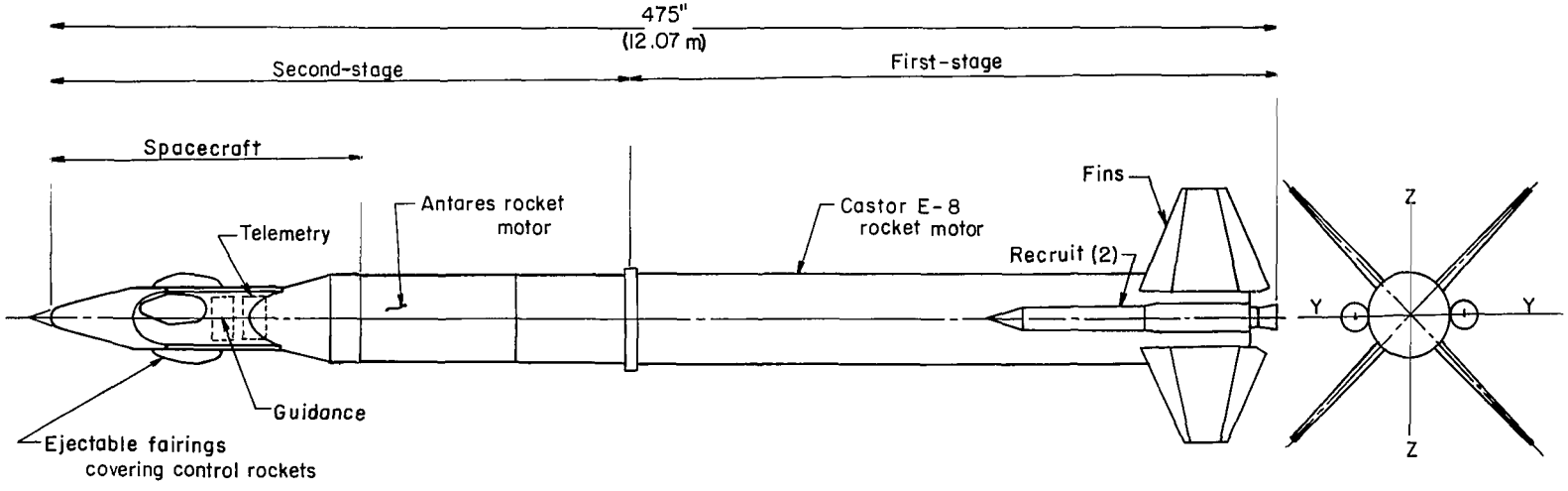

Figure 4.- General configuration of research vehicle.

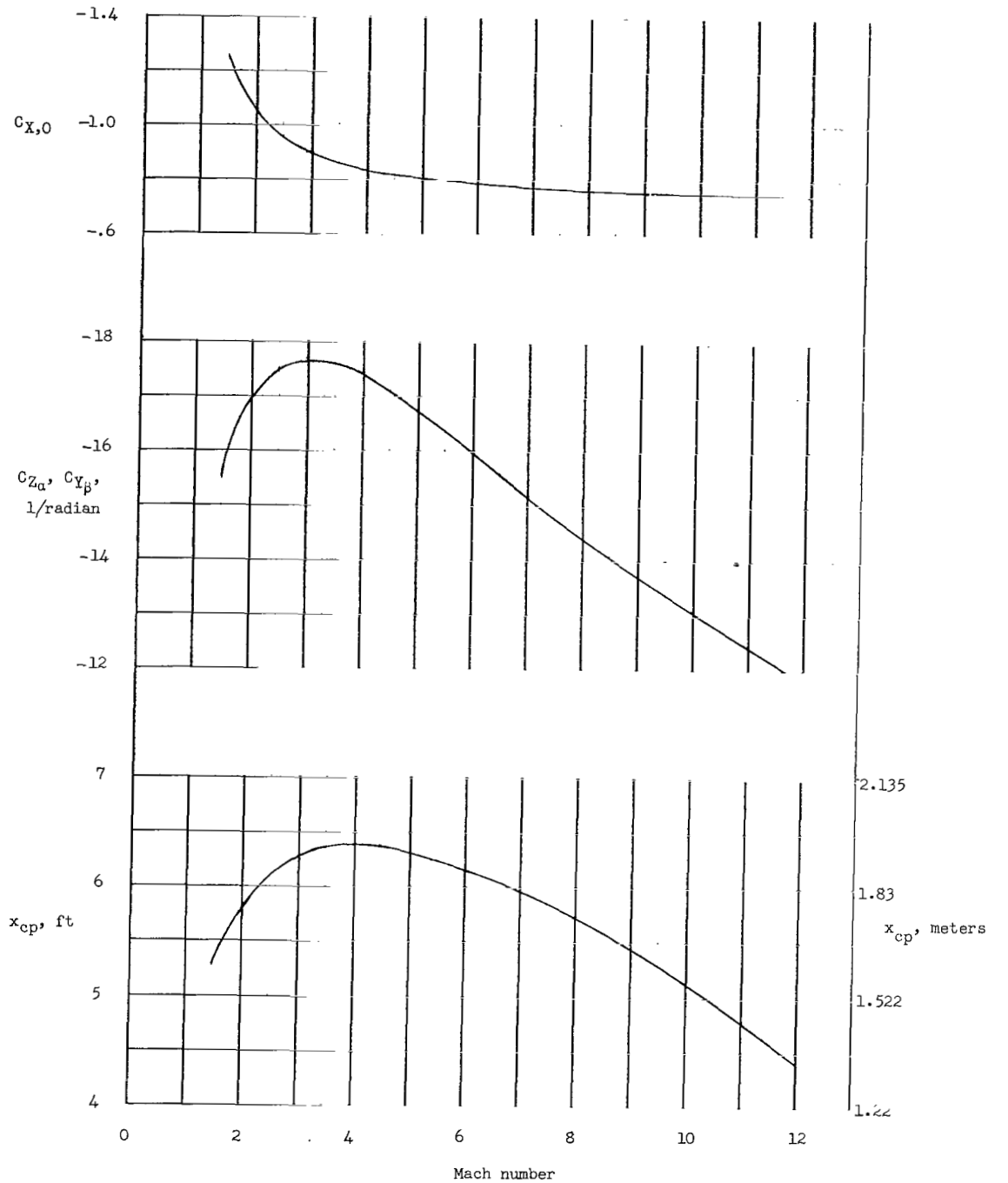

(a) Variation of $C_{X,0}$, C_{Z_α}, C_{Y_β}, and x_{cp} with Mach number.

Figure 5.- Research-vehicle second-stage aerodynamic and physical characteristics.

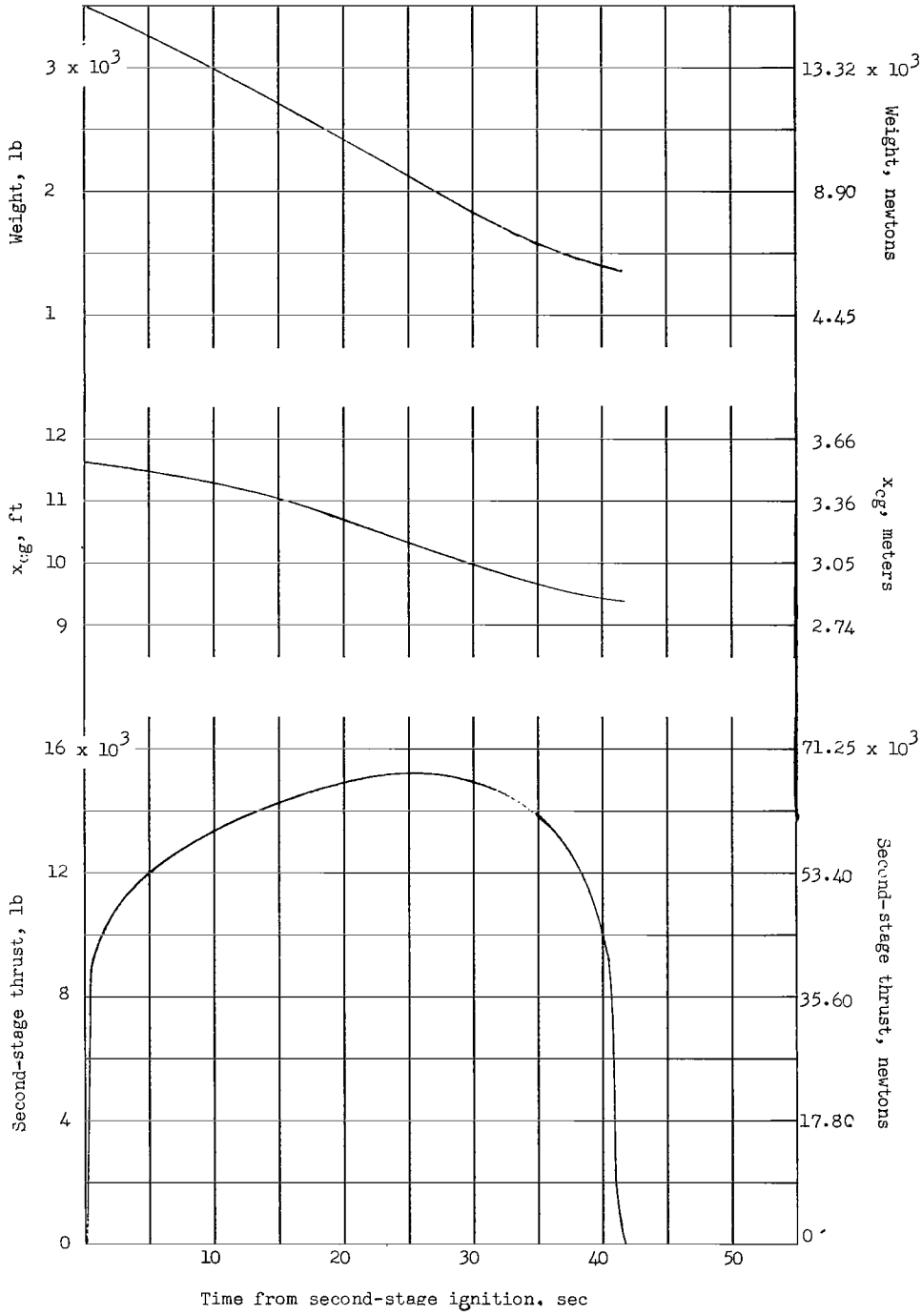

(b) Variation of thrust x_{cg} and weight with time.

Figure 5.- Continued.

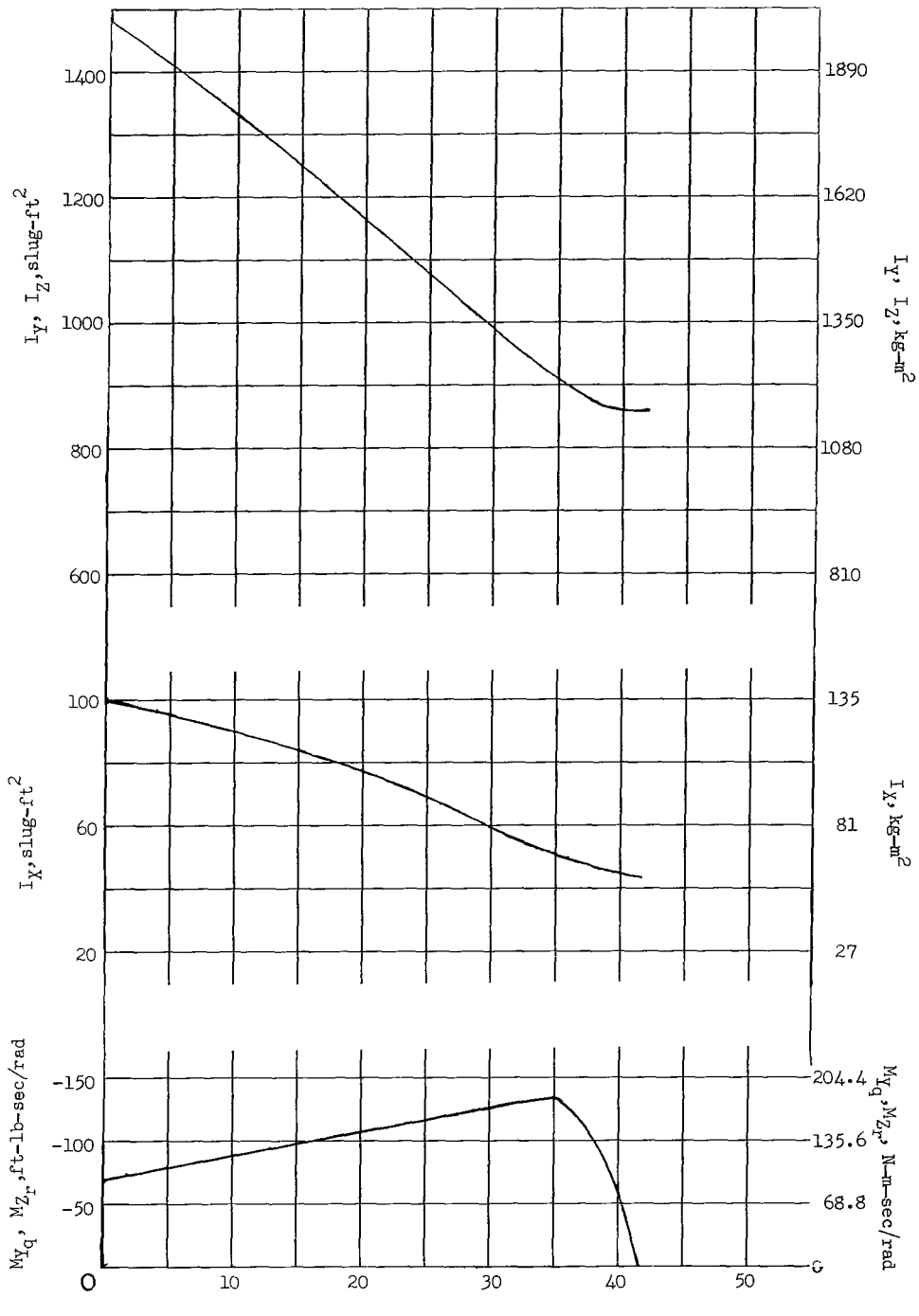

(c) Variation of M_{Y_q}, M_{Z_r}, I_X, I_Y, and I_Z with time.

Figure 5.- Concluded.

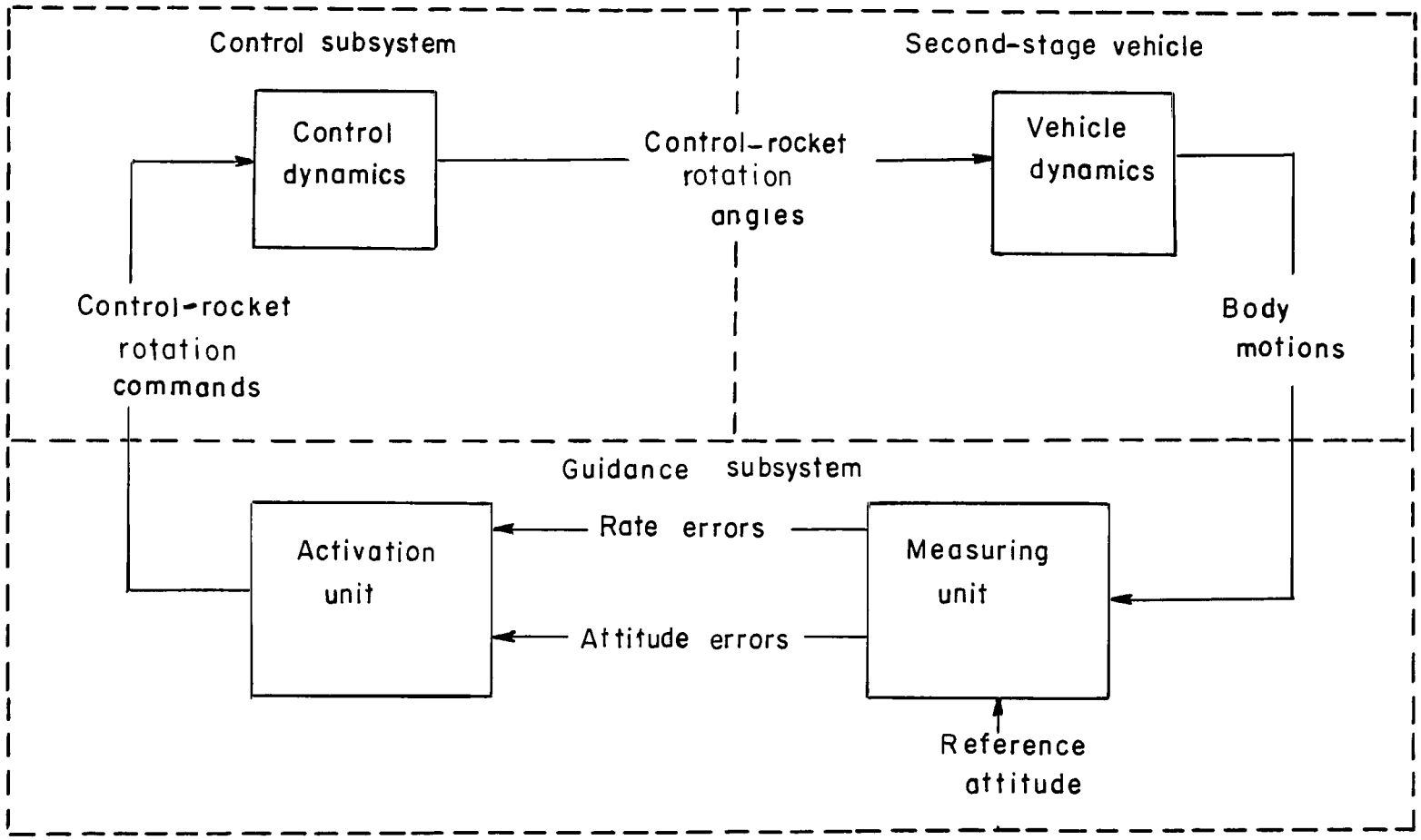

Figure 6.- Block diagram of main elements of second-stage system.

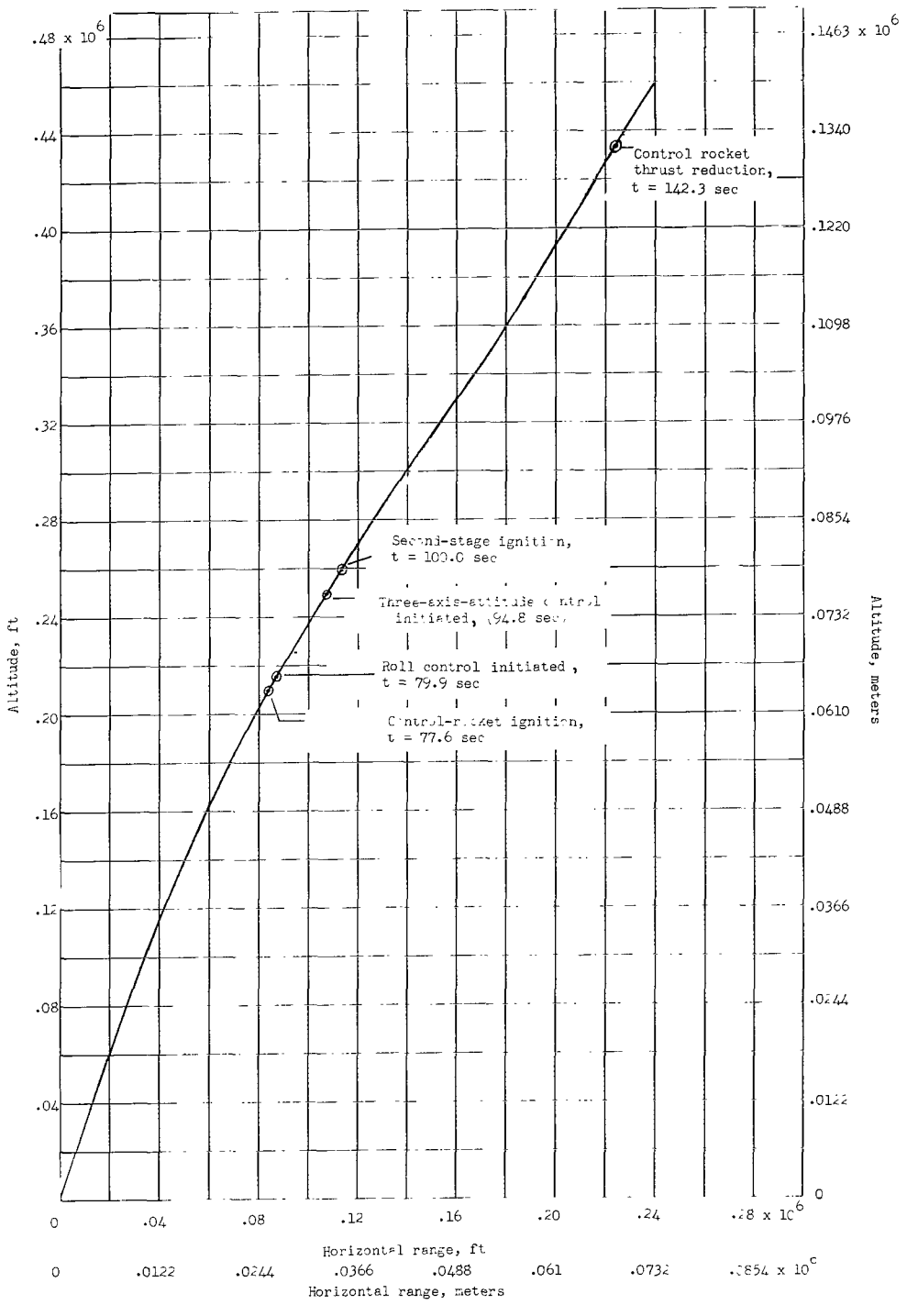

(a) Trajectory in space.

Figure 7.- Research-vehicle trajectory parameters.

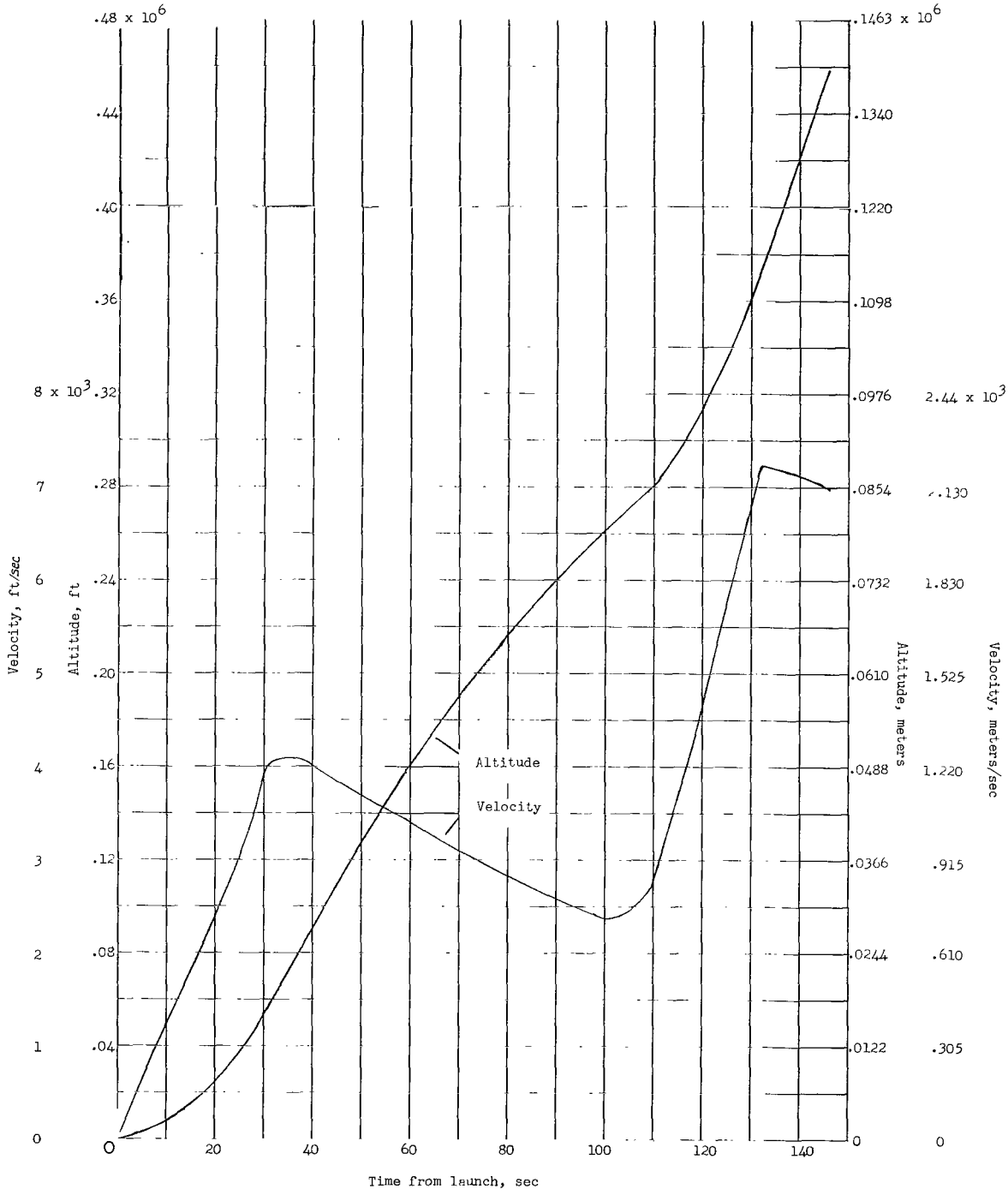

(b) Variation of velocity and altitude with time.

Figure 7.- Concluded.

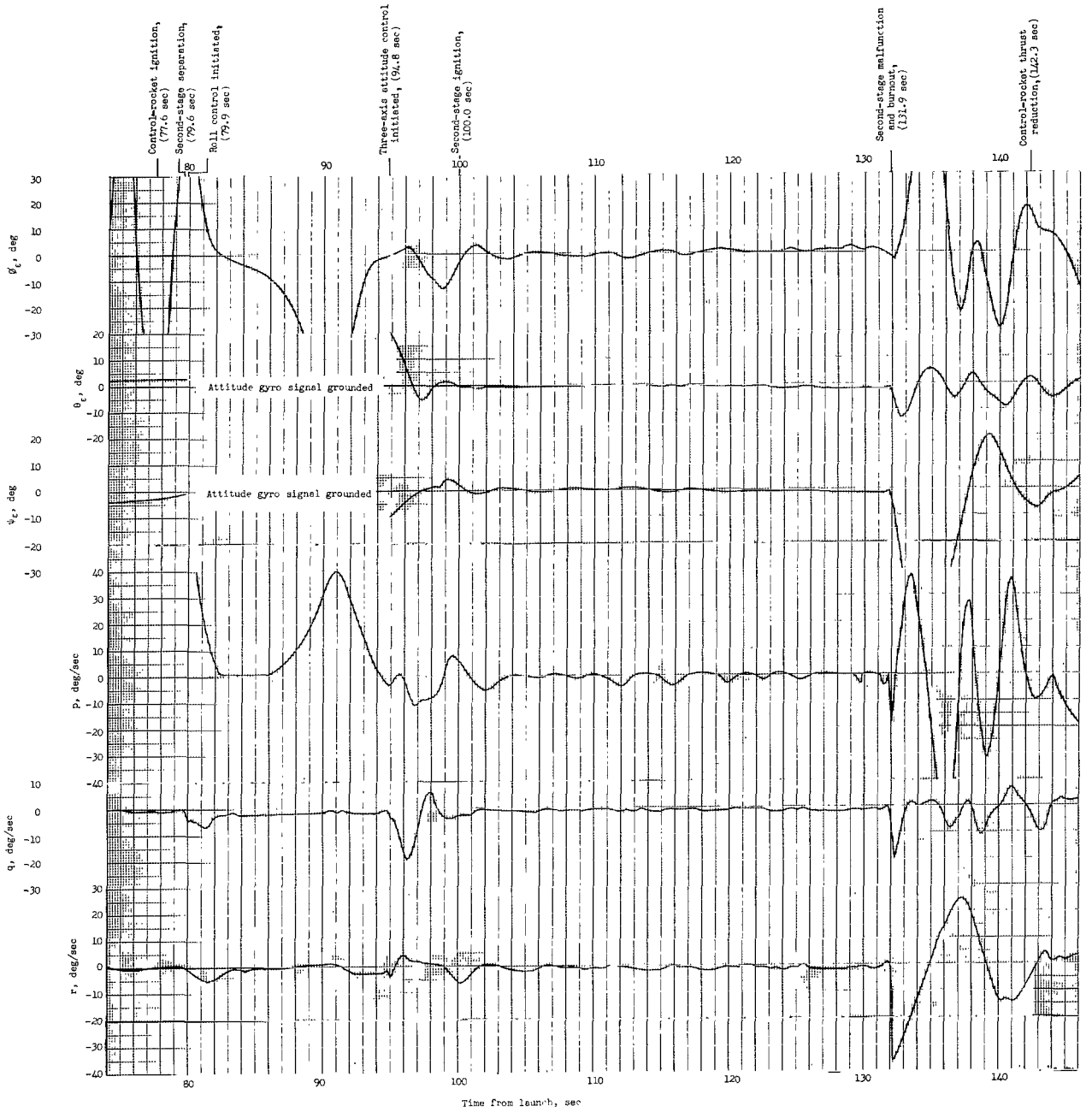

(a) Variation of ψ_ϵ, θ_ϵ, ϕ_ϵ, p, q, and r with time.

Figure 8.- Flight results as obtained from telemetry.

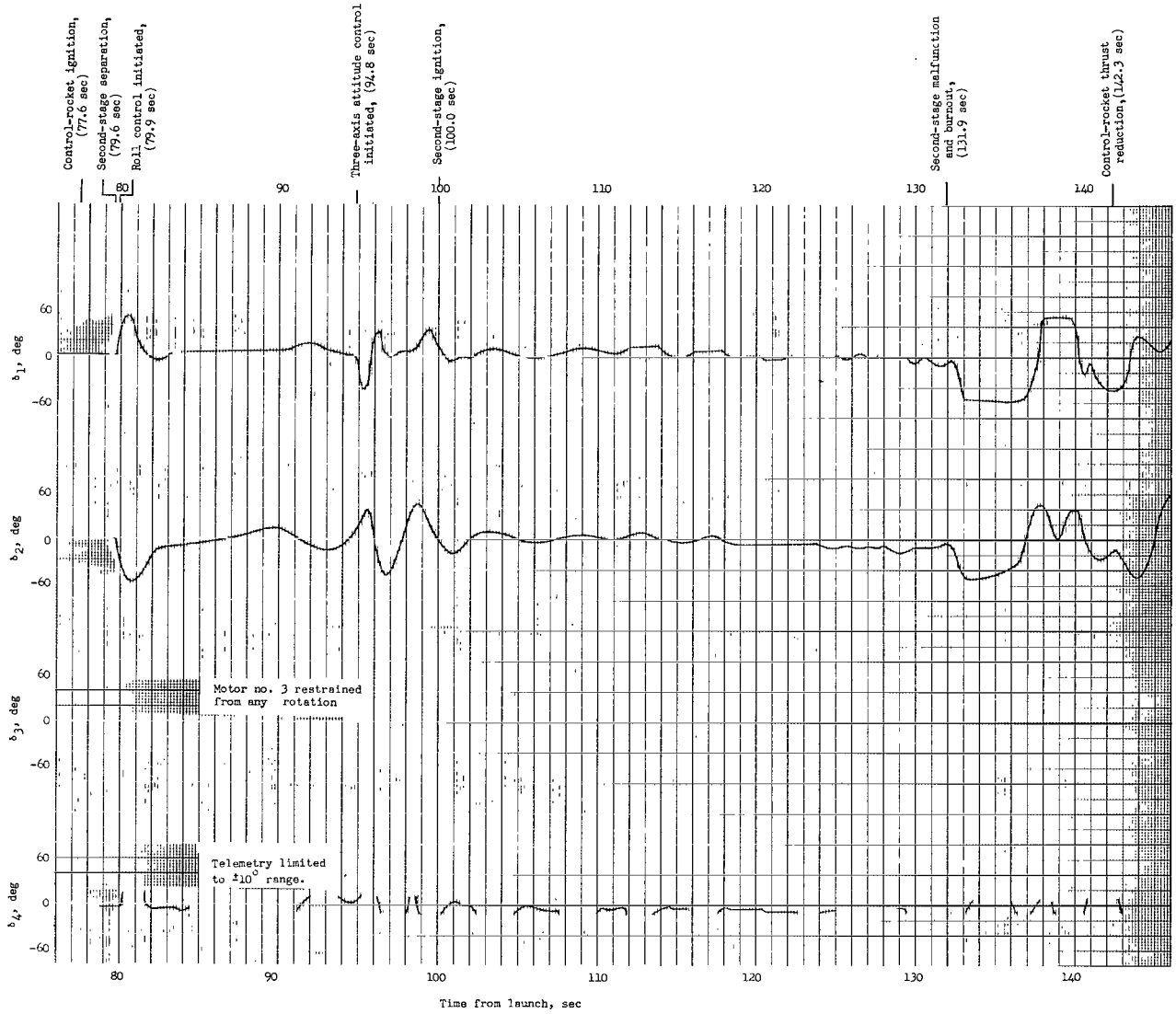

(b) Variation of δ_1, δ_2, δ_3, and δ_4 with time.

Figure 8.- Concluded.

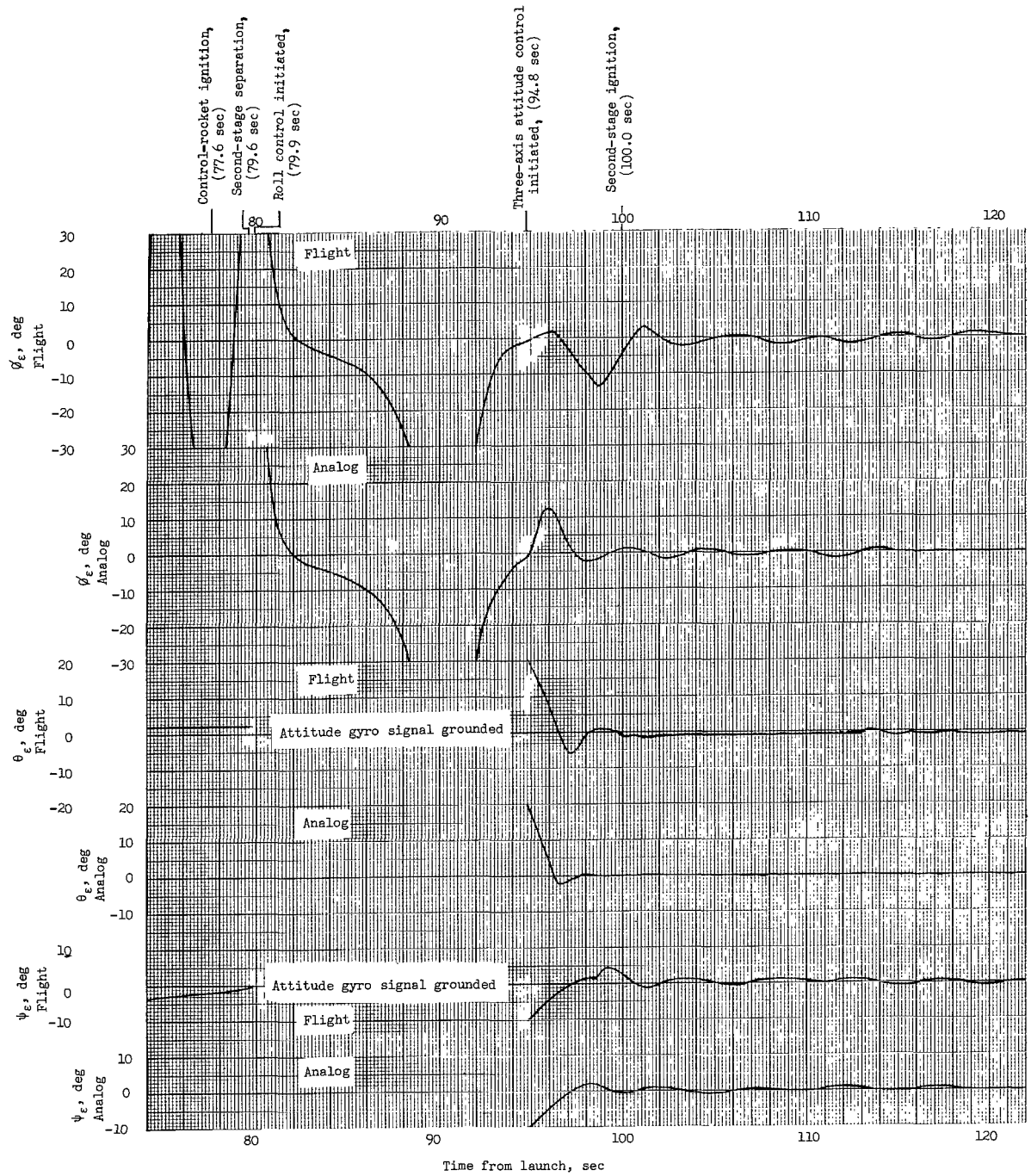

(a) Variation of ψ_ϵ, θ_ϵ, and ϕ_ϵ with time.

Figure 9.- Comparison of flight results with analog simulations for restrained control system.

(b) Variation of p, q, and r with time.

Figure 9.- Concluded.

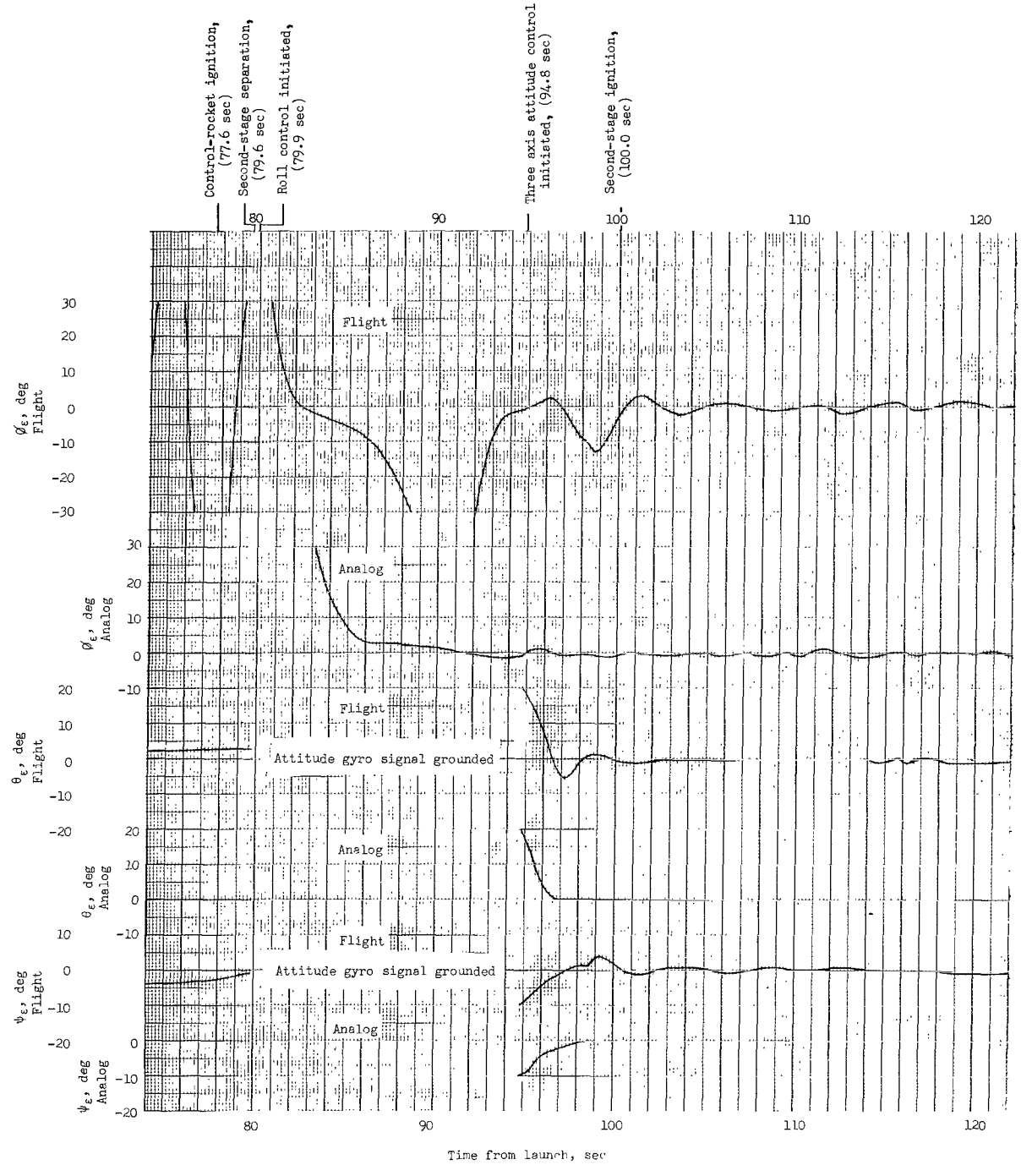

(a) Variation of ψ_ϵ, θ_ϵ, and ϕ_ϵ with time.

Figure 10.- Comparison of flight results with analog simulations for unrestrained control system.

(b) Variation of p, q, and r with time.

Figure 10.- Concluded.

"The aeronautical and space activities of the United States shall be conducted so as to contribute . . . to the expansion of human knowledge of phenomena in the atmosphere and space. The Administration shall provide for the widest practicable and appropriate dissemination of information concerning its activities and the results thereof."

—NATIONAL AERONAUTICS AND SPACE ACT OF 1958

NASA SCIENTIFIC AND TECHNICAL PUBLICATIONS

TECHNICAL REPORTS: Scientific and technical information considered important, complete, and a lasting contribution to existing knowledge.

TECHNICAL NOTES: Information less broad in scope but nevertheless of importance as a contribution to existing knowledge.

TECHNICAL MEMORANDUMS: Information receiving limited distribution because of preliminary data, security classification, or other reasons.

CONTRACTOR REPORTS: Technical information generated in connection with a NASA contract or grant and released under NASA auspices.

TECHNICAL TRANSLATIONS: Information published in a foreign language considered to merit NASA distribution in English.

TECHNICAL REPRINTS: Information derived from NASA activities and initially published in the form of journal articles.

SPECIAL PUBLICATIONS: Information derived from or of value to NASA activities but not necessarily reporting the results of individual NASA-programmed scientific efforts. Publications include conference proceedings, monographs, data compilations, handbooks, sourcebooks, and special bibliographies.

Details on the availability of these publications may be obtained from:

SCIENTIFIC AND TECHNICAL INFORMATION DIVISION

NATIONAL AERONAUTICS AND SPACE ADMINISTRATION

Washington, D.C. 20546